IEEE Access
Multidisciplinary | Rapid Review | Open Access Journal

Received May 21, 2020, accepted May 25, 2020, date of publication May 29, 2020, date of current version June 11, 2020.

Digital Object Identifier 10.1109/ACCESS.2020.2998516

A Full-Band Digital Television Transmitting Antenna Array With Dual-Layer Bowtie Dipole Unit

HAIJING YU, SHAOJUN FANG, (Member, IEEE), LINGLING JIANG, AND HONGMEI LIU, (Member, IEEE)
School of Information Science and Technology, Dalian Maritime University, Dalian 116026, China

Corresponding author: Shaojun Fang (fangshj@dlmu.edu.cn)

This work was supported in part by the National Natural Science Foundation of China under Grant 51809030 and Grant 61871417, in part by the Natural Science Foundation of Liaoning Province under Grant 2020-MS-127, and in part by the Fundamental Research Funds for the Central Universities under Grant 3132020207 and Grant 3132020206.

ABSTRACT A full-band digital television (DTV) transmitting antenna array with dual-layer bowtie dipole unit is proposed in this paper. The dual-layer bowtie dipole is utilized as the antenna unit to broaden the frequency bandwidth, and its key parameters are discussed. Besides, a wideband impedance matching network with stepped complex impedance transformers is designed to achieve the full-band low voltage standing wave ratio (VSWR). For verification, a prototype is designed, fabricated, and measured. The experimental results agree well with the simulations. The measurement shows a relative bandwidth of 62.4% (455 MHz – 868 MHz) under the criterion of VSWR $<$ 1.15. Particularly, the VSWR is less than 1.13 within the range of 470 MHz – 862 MHz, (i.e. the full band of the DTV transmitting system). And the proposed antenna maintains a stable gain larger than 11.6 dBi over the operating frequency band with the half-power beam width of $70°\pm 3°$ in the horizontal plane, which meets the requirements of the full-band signal transmission in the DTV broadcasting system.

INDEX TERMS Full-band antenna array, dual-layer bowtie dipole, DTV transmitting antenna, low VSWR.

I. INTRODUCTION

Digital television (DTV) broadcasting has mostly replaced the conventional analog TV broadcasting due to the advantage of high frequency spectrum utilization and multichannel operation modes [1], [2]. Meanwhile, a series of standards for DTV broadcasting based on the operating band of 470 MHz - 862 MHz were widely adopted by the most of Europe and Asia, such as terrestrial digital video broadcasting (DVB-T), DVB-T2, and digital television terrestrial multimedia broadcasting (DTMB) [3], [4]. As an essential device of DTV transmission system, the transmitting antenna requires the characteristics of broadband, high gain, high power capacity and low voltage standing wave ratio (VSWR), so as to improve the frequency utilization, widen the coverage range, and protect the output stage amplifier from damage [5], [6].

The associate editor coordinating the review of this manuscript and approving it for publication was Davide Comite.

Over the past decades, a variety of classic DTV transmitting antenna implementations have been proposed, such as ring loop antennas [7], [8] and modified batwing antennas [9]–[11]. Since simple feeding structures are employed, these wideband antennas with high gains are widely applied in the early DTV system. To obtain the VSWR less than 1.15, a balance to unbalance feeding structure [12] is utilized to achieve the relative bandwidth of 40%. In [13], a stacked E-shaped patch is designed to achieve a lower profile. Meanwhile, the VSWR can maintain lower than 1.15 over the frequency range from 544 MHz to 653 MHz. However, the peak gain of 9.23 dBi is inferior to the aforementioned methods, and the microstrip structure cannot suffer from high transmitting power. Thus, several antennas with different operating frequencies are needed to cover the full band of 470 MHz – 862 MHz, which results in a higher cost.

In order to broaden the operating bandwidth much further, several dipole antennas for DTV transmitting are

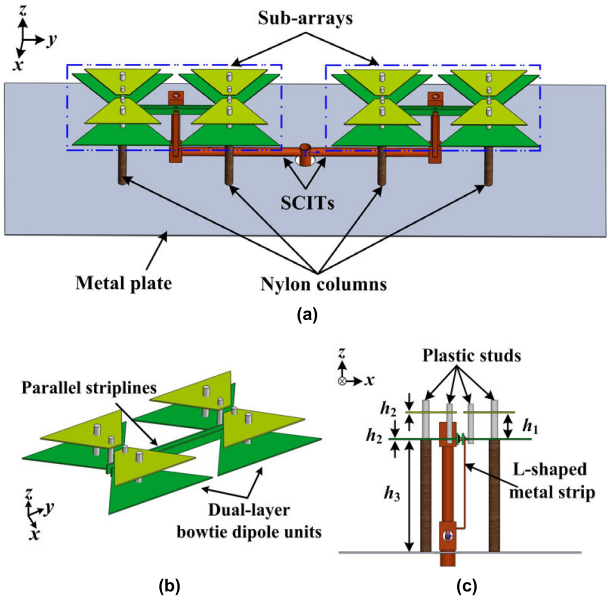

FIGURE 1. Geometry of the proposed antenna array. (a) Structure of the antenna. (b) Geometry of sub-array. (c) Side view.

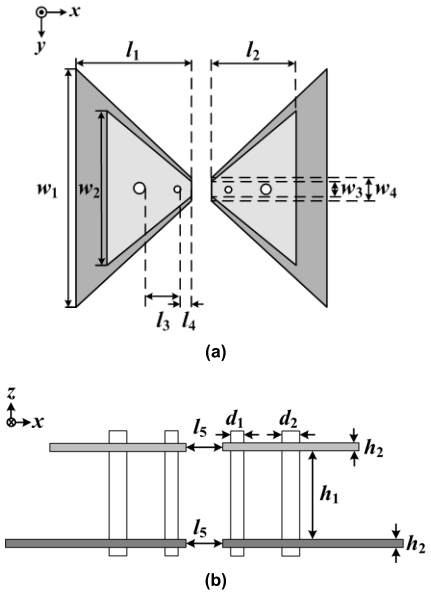

FIGURE 2. Geometry of the dual-layer bowtie dipole unit. (a) Top view. (b) Side view.

proposed [14]–[16]. In the papers [14], [15], two stereoscopic antennas with compensated baluns are introduced. By using the modified baluns, the relative bandwidths under VSWR < 1.15 are enhanced to 37.2% and 44.6%. In [16], a bowtie antenna with incision gap is proposed. Due to the wideband antenna unit, the relative bandwidth reaches 77.1% under the VSWR < 2, and the high gains are 13.4 dBi - 16.1 dBi within the frequency range of 470 MHz - 862 MHz. Unfortunately, these antennas still cannot satisfy with the requirement for VSWR < 1.15 within the full band (470 MHz – 862 MHz).

In this paper, a full-band antenna array with low VSWR is proposed for DTV transmission system. The proposed antenna array is composed of the dual-layer bowtie dipole units. Due to the utilization of the dual-layer antenna unit, the operating frequency range of the antenna array covers the full-band of the DTV transmitting system (470 MHz – 862 MHz) completely. A wideband matching network is designed with stepped complex impedance transformers (SCIT) to achieve low VSWR. Furthermore, high gains and stable radiation performances of the antenna array are obtained simultaneously with horizontal polarization.

The content of the paper is organized as follows: Section II provides the structure of the proposed antenna array unit and the matching network and the key parameters are discussed in detail. The experimental results are illustrated in section III, followed by a conclusion in section IV.

II. DESIGN OF THE PROPOSED FULL-BAND DTV TRANSMITTING ANTENNA ARRAY

The configuration of the proposed antenna is shown in Fig. 1(a). It consists of two sub-arrays, a wideband matching network, and a metal plate as the reflecting ground. It can be seen in Fig. 1(b) that the sub-array is composed of two dual-layer bowtie dipole units and a transmission line made of a pair of parallel striplines. Two SCITs are employed in the matching network to benefit the improvement of antenna bandwidth. Fig. 1(c) shows the side view of this design on the xoz plane. The lower and upper bowtie dipoles are connected by the plastic studs, and the whole antenna is supported by eight nylon columns. Besides, an L-shaped metal strip is used as a balun to achieve balance to unbalance conversion.

A. DESIGN OF THE ANTENNA UNIT

Fig. 2 shows the geometry of the dual-layer bowtie dipole unit which adopts a dual-layer gradual structure to extend the current path and realize a wide band. The upper and lower bowtie dipoles are fixed by four plastic studs. A parametric study has been carried out in this initial stage to identify the optimal dimensions. In order to obtain the full-band radiation, the single arm lengths of $l_1 = 113$ mm $(0.25\lambda_0)$, $l_2 = 87$ mm $(0.25\lambda_H)$ and the widths of $w_1 = 226$ mm $(0.5\lambda_0)$, $w_2 = 174$ mm $(0.5\lambda_H)$, $w_3 = 25$ mm $(0.07\lambda_H)$, $w_4 = 30$ mm $(0.07\lambda_0)$ are determined according to λ_0 and λ_H, where $\lambda_0 = 450$ mm and $\lambda_H = 348$ mm are the wavelengths respectively corresponding to $f_0 = 665$ MHz and $f_H = 862$ MHz. The height between the upper and lower dipole is identical as $h_1 = 43$ mm $(0.1\lambda_0)$. Two different plastic studs with diameters of $d_1 = 8$ mm and $d_2 = 10$ mm are drilled on the single arm, where the two studs are located with the distance of $l_3 = 42.5$ mm and $l_4 = 10$ mm. The distance between the two arms is $l_5 = 20$ mm. The thickness of all metal dipoles is $h_2 = 2$ mm.

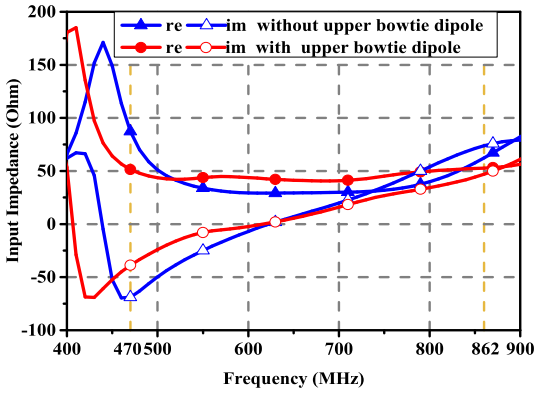

FIGURE 3. Effect of the upper bowtie dipole.

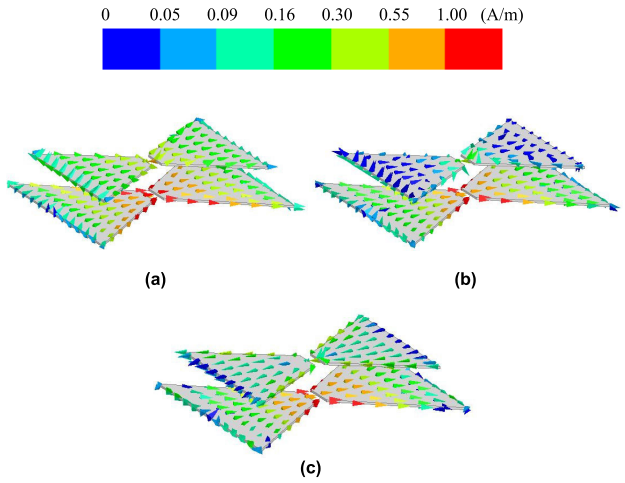

FIGURE 4. The normalized current distribution of the antenna unit at (a) 500 MHz, (b) 665 MHz, (c) 800 MHz.

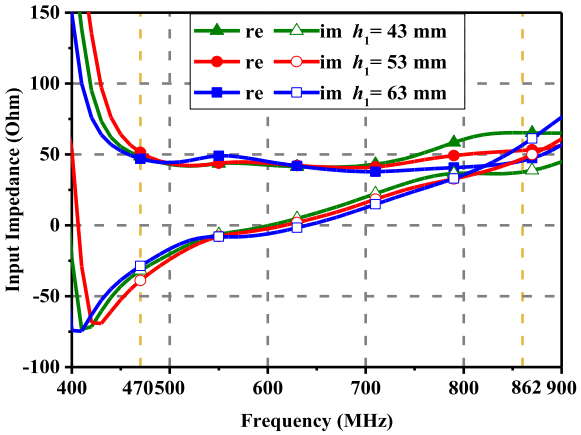

FIGURE 5. Effect of the simulated input impedance for different h_1 between the upper and lower bowties.

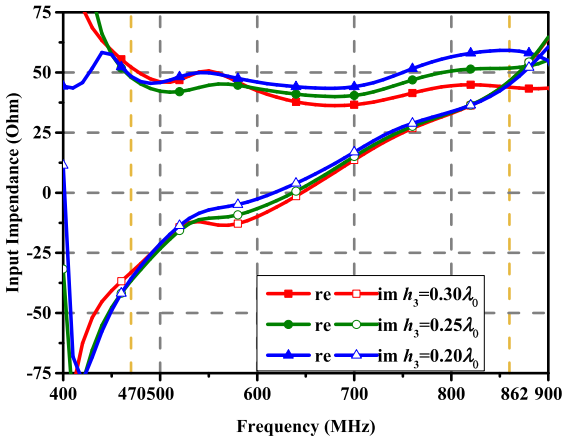

FIGURE 6. The simulated input impedance for different h_3.

The influence of dimension parameters on performance is discussed in the following part. As shown in Fig. 3, the variation range of input reactance reduces obviously after employing the upper bowtie dipole. Meanwhile, the input resistance is much flatter around 50 Ω within the full band owing to the upper bowtie dipole. Thus, the impedance bandwidth can be enhanced obviously by the structure of dual-layer bowtie dipole.

Fig. 4 illustrates the current distributions of the antenna unit. At the center frequency of 665 MHz, the current is mainly distributed on the lower dipole. At the lower and upper operating frequency of 500 MHz and 800 MHz, the surface currents are significantly increased along the upper dipole, thereby resulting in a wider impedance bandwidth.

Fig. 5 depicts the simulated input impedance of the antenna unit for different values of h_1. It can be seen that the real part of the input impedance for the upper frequency band decreases sensitively with the increasing of h_1, while for the lower frequency band, the real part of the input impedance can maintain consistent with different values of h_1. Besides, the h_1 has a slight effect on the imaginary part of the input impedance for the full operating band.

Fig. 6 gives the effect of the height of h_3 from the lower dipole to the ground. It is observed that the input resistance decreases with the increasing h_3, especially for the upper frequency band, whereas the input reactance has slight changes for different h_3.

Fig. 7(a) shows the simulated input impedance for different values of l_1. The real part of the input impedance decreases with the increasing of l_1, while the variation range of the imaginary part rises within the full band. The l_2 mainly make an effect on the upper frequency band of 750 MHz – 862 MHz, which can be seen in Fig. 7(b). The imaginary part of the input impedance has an obvious reduction with the increasing of l_2, while the real part increases within the upper band. Hence, compromising the real and imaginary part of the input impedance and choosing the appropriate l_1 and l_2, the impedance bandwidth can be widened obviously.

B. DESIGN OF THE MATCHING NETWORK

The antenna array employs two sub-arrays which are composed of two antenna units to improve the gains within the full band. In order to support the operation of the antenna

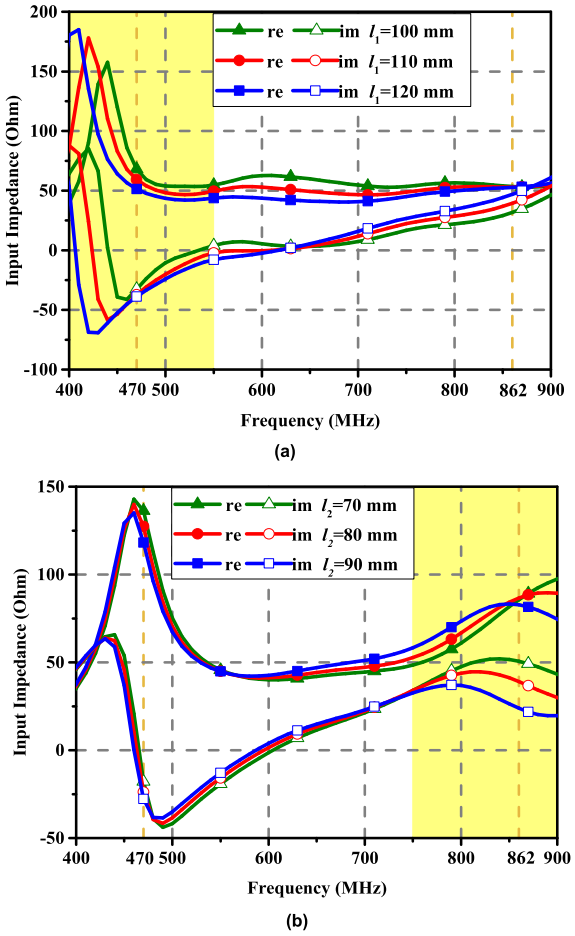

FIGURE 7. Simulated input impedance for different l_1 and l_2. (a) Simulated input impedance for different l_1. (b) Simulated input impedance for different l_2.

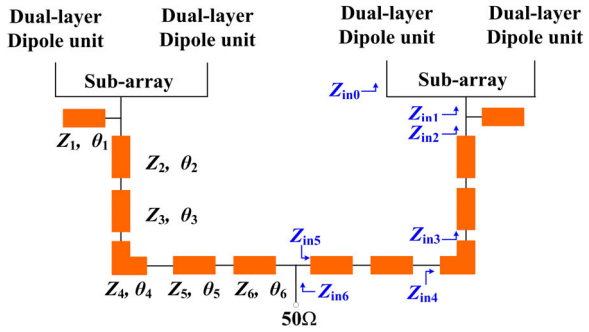

FIGURE 8. Schematic of the wideband matching network.

units, a T-shaped matching network is used. Since the input impedance is regulated at 50 Ω, the input impedance of the sub-array needs to be matched to 100 Ω in the full band. Furthermore, to improve the radiation patterns and peak gains in the full band, the distance between adjacent dual-layer dipole units is expected to be $0.5\lambda_0$ [17].

The multi-section structure is used to achieve the full-band matching network. Fig. 8 shows the schematic of the wideband matching network which is composed of two SCITs with six different transmission lines. The six different transmission lines (TL$_i$, $i = 1, 2, \ldots, 6$) have the characteristic impedance Z_i and electrical length θ_i.

Since $Z_{\text{in1}}(f)$ is a variable complex impedance as a function of f, the parallel TL$_1$ is firstly introduced to compensate the input reactance of $Z_{\text{in1}}(f)$, and the $Y_{\text{in2}}(f)$ is obtained mathematically in (1).

$$Y_{\text{in2}}(f) = Y_{\text{in1}}(f) + \text{j}Y_1 \cot[\theta_1(f)], \tag{1}$$

where the $Y_{\text{in1}}(f)$, $Y_{\text{in2}}(f)$ and Y_1 are the reciprocals of $Z_{\text{in1}}(f)$, $Z_{\text{in2}}(f)$ and Z_1, respectively. The $Y_{\text{in1}}(f)$ is given as (2).

$$Y_{\text{in1}}(f) = G_{\text{in1}}(f) + \text{j}B_{\text{in1}}(f), \tag{2}$$

In order to compensate the input susceptance of $Y_{\text{in1}}(f)$, the $Y_1 \cot[\theta_1(f)]$ is expected to be equal to $-B_{\text{in1}}(f)$ near f_0. Meanwhile, the input reactance of $Z_{\text{in2}}(f)$ becomes flatter by adding the TL$_1$ in parallel.

Secondly, two transmission lines TL$_2$ and TL$_3$ are designed to match $Z_{\text{in2}}(f)$ to be around 50 Ω. The electrical length of each transmission lines θ_2 and θ_3 are equal to $(\pi/4)$ at f_0 to promise the total length to be $(\pi/2)$.The expression of $Z_{\text{in3}}(f)$ can be equated in (3).

$$Z_{\text{in3}}(f) = Z_3 \frac{Z_{\text{in2}}(f)\left[Z_2 - Z_3\tan^2\left(\frac{\pi f}{4f_0}\right)\right] + \text{j}Z_2(Z_2+Z_3)\tan\left(\frac{\pi f}{4f_0}\right)}{Z_2\left[Z_3 - Z_2\tan^2\left(\frac{\pi f}{4f_0}\right)\right] + \text{j}Z_{\text{in2}}(f)(Z_2+Z_3)\tan\left(\frac{\pi f}{4f_0}\right)} \tag{3}$$

where the $Z_{\text{in3}}(f)$ is expected around 50 Ω.

In order to realize lower VSWR, another part of multi-section matching is designed to transform $Z_{\text{in4}}(f)$ to be around 100 Ω with TL$_5$ and TL$_6$, which designate the quarter-wavelength transmission lines with the total length of π. The $Z_{\text{in5}}(f)$ can be obtained from (4).

$$Z_{\text{in5}}(f) = Z_6 \frac{Z_{\text{in4}}\left[Z_5 - Z_6\tan^2\left(\frac{\pi f}{2f_0}\right)\right] + \text{j}Z_5(Z_5+Z_6)\tan\left(\frac{\pi f}{2f_0}\right)}{Z_5\left[Z_6 - Z_5\tan^2\left(\frac{\pi f}{2f_0}\right)\right] + \text{j}Z_4(f)(Z_5+Z_6)\tan\left(\frac{\pi f}{2f_0}\right)} \tag{4}$$

where

$$Z_{\text{in4}}(f) = Z_4 \frac{Z_{\text{in3}}(f) + \text{j}Z_4\tan[\theta_3(f)]}{Z_4 + \text{j}Z_{\text{in3}}(f)\tan[\theta_3(f)]} \tag{5}$$

where $Z_4 = 50\Omega$ is the characteristic impedance of TL$_4$, which is employed for the corner connecting.

The $Z_{\text{in6}}(f)$ can be determined after two six-section complex impedance transformers connected in parallel, as shown in (6).

$$Z_{\text{in6}}(f) = \frac{Z_{\text{in5}}(f)}{2} \tag{6}$$

In the ideal case, the condition of full-band matching standard of 50 Ω should be satisfied as (7).

$$|Z_{\text{in6}}(f) - 50| < \varepsilon, \quad f \in [470\text{MHz}, \quad 862\text{MHz}] \tag{7}$$

where ε is expected to approach zero.

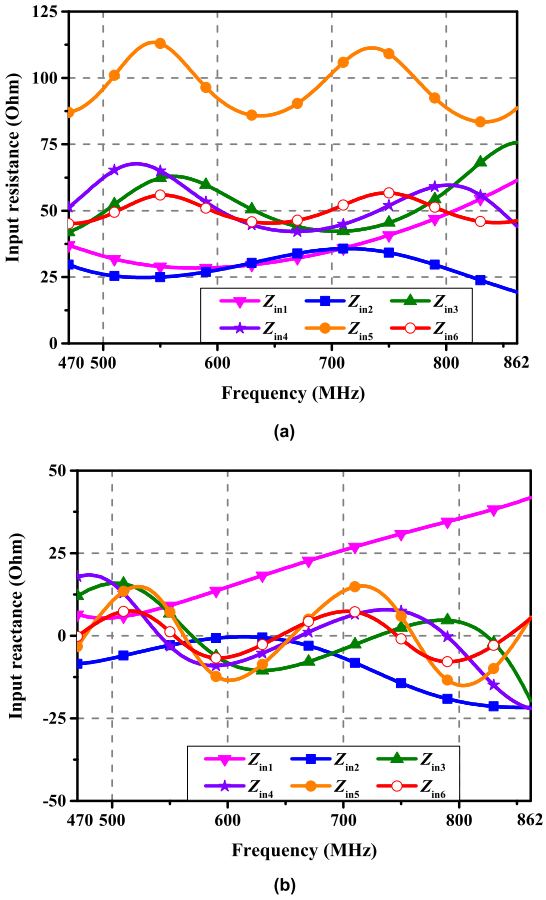

FIGURE 9. Simulated results of the input resistance and reactance. (a) Simulated input resistance. (b) Simulated input reactance.

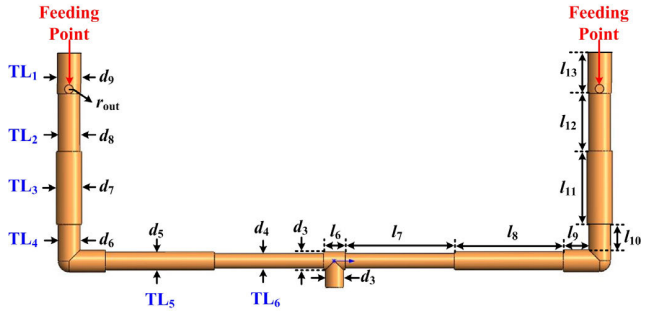

FIGURE 10. Geometry of the matching network.

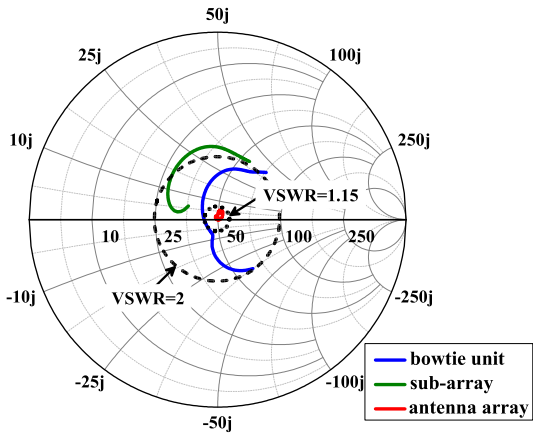

FIGURE 11. Simulated input impedance (470 MHz – 862 MHz) shown in Smith chart.

The parameters of the transmission lines can be arranged with the help of the Advanced Design System simulator. The optimized parameters of six transmission lines are summarized as follows: $Z_1 = 34\ \Omega$, $Z_2 = 53\ \Omega$, $Z_3 = 37\ \Omega$, $Z_5 = 66\ \Omega$, $Z_6 = 91\ \Omega$, $\theta_1 = 31°$, and $\theta_4 = 18°$.

Fig. 9 gives the real and imaginary part of the input impedance $Z_{\text{in}i}(i = 1, 2, \ldots, 6)$. It revealed that the reactance of $Z_{\text{in}1}$ is sensitive to different frequencies. By connecting the TL_1 in parallel, the reactance of $Z_{\text{in}1}$ is compensated to j0 near f_0 and the flatter reactance is obtained in the full band. The resistance of $Z_{\text{in}3}$ flattens around 50 Ω within a wide band from 470 MHz - 800 MHz due to two transmission lines of TL_2 and TL_3. But the changes of the input impedance cannot satisfy the VSWR < 1.15 within the full band. Hence, the other parts of the multi-section matching network are needed to further decrease the VSWR. It can be observed that the TL_4 has a slight influence on both the input resistance and reactance from $Z_{\text{in}3}$ to $Z_{\text{in}4}$. After the impedance transformation of the TL_5 and TL_6, the resistance and reactance of $Z_{\text{in}5}$ drift around 100 Ω and j0 respectively within the full band. Finally, comparing to the $Z_{\text{in}1}$, the imaginary part of $Z_{\text{in}6}$ has less fluctuation around j0, and the real part has less fluctuation around 50 Ω within the full band due to the multi-section matching network and the parallel connection of the SCITs.

Considering the actual engineering requirement of high power capacity, the coaxial line is used to realize the matching network. Fig. 10 illustrates the geometry of the inner conductor of the coaxial line, while the radius of the outer conductor is 10mm. In the actual application, the mutual coupling is increased by the compactness of the sub-array and the antenna array, which leads to poor impedance and radiation performance [18]. But the influence on the mutual coupling is ignored in the theoretical analysis. Thus, the physical parameters need to be optimized much further.

By fixing the outer conductor radius and adjusting the inner conductor radius, the optimal parameters can be achieved with the help of the Ansoft HFSS simulator. The optimized dimensions are listed in Table 1. Fig. 11 indicates the matching improvement of the antenna array in the Smith chart. The VSWR of the bowtie unit is almost less than 2, and the input impedance of the sub-array shows an obvious inductive character in the full band. However, after integrating and adjusting the parameters of the matching network, the input impedance of the antenna array is around 50 Ω, which shows the VSWR is less than 1.15 within the full band. Thus, the transmitting antenna array achieves full-band matching by utilizing the wideband matching network on the basis of ensuring the dimension of the antenna array.

TABLE 1. The optimal dimensions of the antenna array (Unit: mm).

l_1	l_2	l_3	l_4	l_5	l_6	l_7
113	75	42.5	10	21	12	113
l_8	l_9	l_{10}	l_{11}	l_{12}	l_{13}	d_1
108	10	12	48	53	40	8
d_2	d_3	d_4	d_5	d_6	d_7	d_8
10	7	3.5	5.4	6.5	8	6.2
d_9	r_{out}	w_1	w_2	w_3	w_4	h_1
9	2.35	180.5	153	27.5	30	38

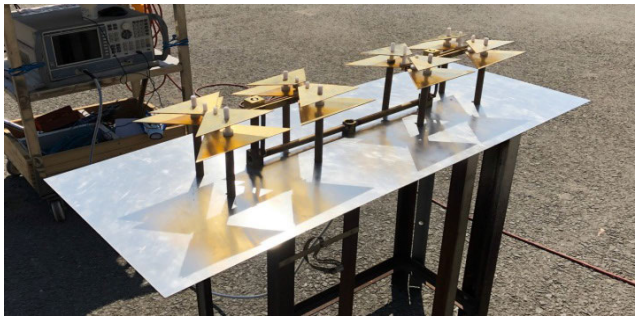

FIGURE 12. The photograph of the fabricated antenna array.

III. IMPLEMENTATION AND PERFORMANCE

The prototype of the proposed antenna array is made, and its photograph is shown in Fig. 12. The overall size of this prototype is $2.67\lambda_0 \times \lambda_0 \times 0.34\lambda_0$. Every two dual-layer bowtie dipole units are connected with a pair of striplines. Each stripline has a dimension of 256 mm × 15 mm. The nylon columns with the radius of 8 mm and the height of 113 mm are used. The L-shaped metal strip has the total length of 100 mm. And all the metal structures have the thickness of 2 mm. Finally, the fabricated prototype was measured with an Agilent N5230A network analyzer.

The simulated and measured VSWR of the prototype is depicted in Fig. 13. The measurement shows a relative bandwidth of 62.4% (455 MHz – 868 MHz) under the criterion of VSWR < 1.15. Especially, for the frequency range of 458 MHz – 865 MHz, the VSWR is less than 1.13. The measured relative bandwidth under the criterion of VSWR < 1.15 is narrower than the simulated one (i.e. 67.7%), which is mainly due to the limitation of machining accuracy.

Fig. 14 shows the simulated and measured gains of the prototype versus frequency. As can be seen, the measured gain can reach the peak value of 13.1 dBi at the frequency of 650 MHz. Besides, the gain is larger than 11.6 dBi within the full band.

To illustrate the radiation performance in detail, the simulated and measured radiation patterns at f = 500 MHz, 665 MHz, and 800 MHz are depicted in Fig. 15. Good consistent has been obtained between the simulations and measurements. The measured half-power beam width (HPBW) in the

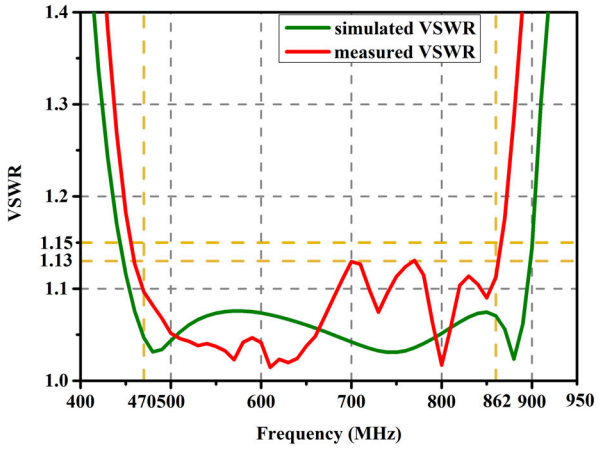

FIGURE 13. Simulated and measured VSWR of the proposed antenna array.

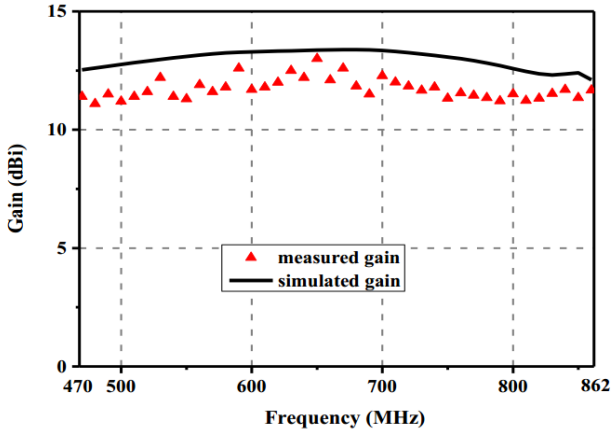

FIGURE 14. Simulated and measured peak gain of the proposed antenna array.

xoz plane at f = 500 MHz, 665 MHz, and 800 MHz are 67.4°, 66.5°, and 73°, respectively, as shown in Fig. 15 (a), (c), (e). The corresponding values in the yoz plane are 30.3°, 22.3°, and 22.7°, respectively, as shown in Fig. 15 (b), (d), (f). The apparent sidelobe of the yoz plane is mainly due to the larger width of the bowtie dipole unit and the coupling effect. These results demonstrate that the proposed antenna meets the requirement of DTV transmitting for a full band, high gain, and low VSWR [19], [20].

Table 2 summarizes the performance comparison between the proposed prototype and previously reported antenna for the DTV transmitting. The proposed antenna shows the widest relative bandwidth compared with other designs for the VSWR < 1.13. In the item of peak gain, the proposed antenna is larger than the antenna in [7], [11]–[14]. For the HPBW in the xoz plane at the center frequency, this design shows the wider HPBW in the xoz plane than the others, which can cover a broader area. In terms of size, the prototype proposed in this paper is almost the same as that in [12], [14], [15], but its performance is much better

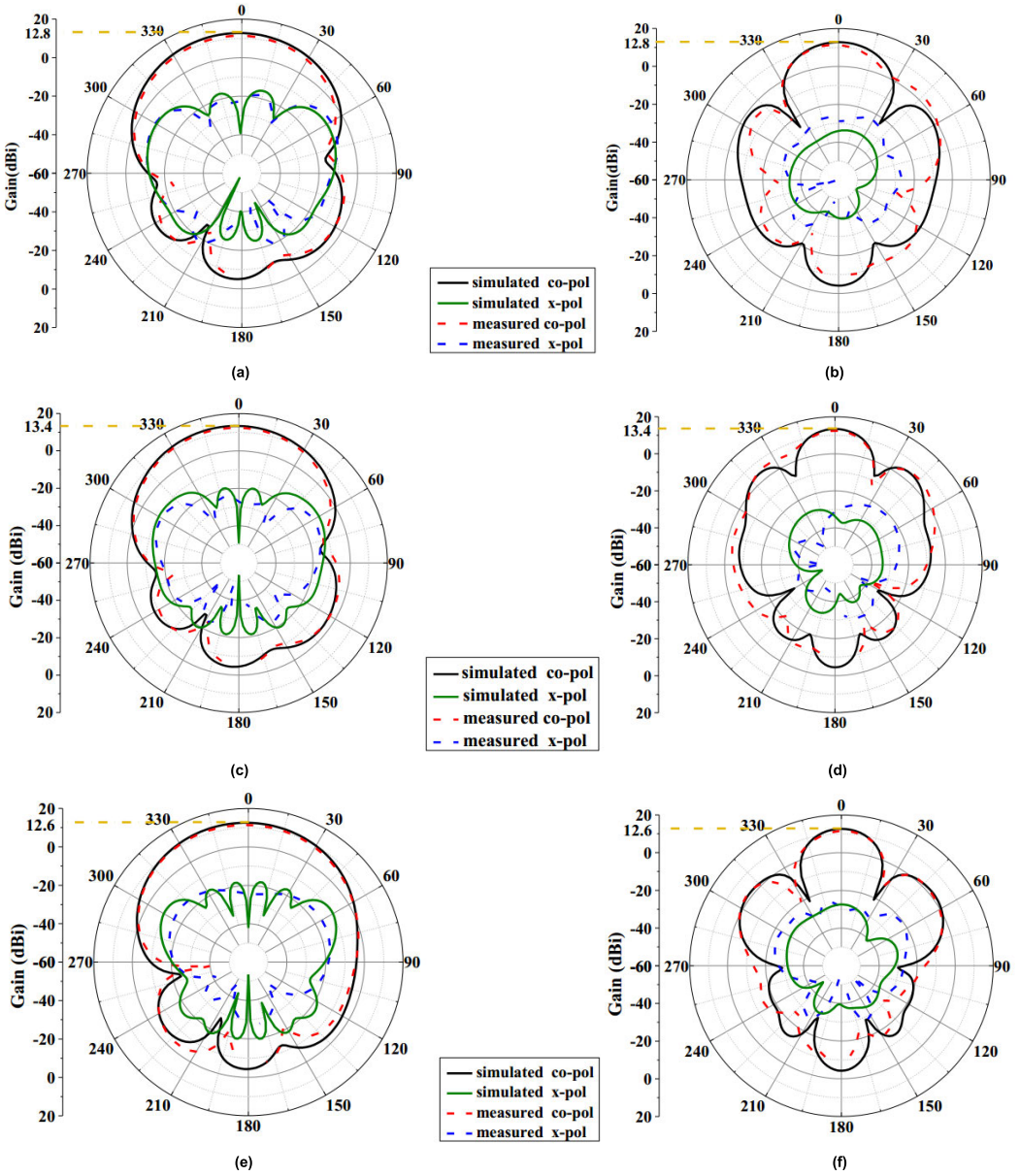

FIGURE 15. The radiation pattern of the proposed antenna for (a) xoz plane at 500 MHz, (b) yoz plane at 500 MHz, (c) xoz plane at 665MHz, (d) yoz plane at 665MHz, (e) xoz plane at 800 MHz, (f) yoz plane at 800 MHz.

TABLE 2. Comparison between this work and previously reported antennas.

Ref.	Frequency Range (MHz)	VSWR[a]	Relative Bandwidth (%)	Gain[b] (dBi)	HPBW[c] (°)	Size ($\lambda_0 \times \lambda_0 \times \lambda_0$)
[7]	575 - 650	1.15	12.2	8.00	NA	NA
[11]	450 - 640	1.15	35.5	11.2	NA	NA
[12]	415 - 607	1.15	37.5	11.2	NA	3.03 × 0.83 × 0.25
[13]	544 - 653	1.15	18.2	8.96	64	0.74 × 0.64 × 0.14
[14]	537 - 850	1.15	45.1	10.0	65	2.23 × 1.07 × 0.42
[15]	600 - 864	1.15	36.1	11.8	62	2.35 × 1.13 × 0.44
This work	458 - 865	1.13	61.5	11.6	66.5	2.67 × 1.00 × 0.34

[a] The maximum value within the frequency band.
[b] The minimum value within the frequency band.
[c] The value in the xoz plane at the center frequency.

than other literature. Although the antenna size in the reference [13] is small, its bandwidth and gain are far lower than other antennas. Hence, this proposed antenna is a good candidate in the application of DTV transmitting.

IV. CONCLUSION

In this paper, a full-band DTV transmitting antenna array is proposed, which uses a dual-layer bowtie dipole as the antenna unit. Its configuration is given, and the related key parameters are discussed. Besides, the structure of the matching network for the full band is illustrated in detail. To verify the feasibility of the proposed antenna, an experiment of this design is investigated. The measurements show that the relative bandwidth of 61.5% for VSWR $<$ 1.13 (458 MHz – 865 MHz) is achieved and the gain within the full band is larger than 11.6 dBi which shows the proposed antenna can be used for the full-band DTV transmitting. As so far, the DTV transmitting antenna with VSWR $<$ 1.13 for the full band has not been found. So the proposed prototype is expected to have a very broad prospect in the DTV transmitting.

REFERENCES

[1] O. T.-C. Chen and C.-Y. Tsai, "CPW-fed wideband printed dipole antenna for digital TV applications," *IEEE Trans. Antennas Propag.*, vol. 59, no. 12, pp. 4826–4830, Dec. 2011.

[2] A. Barrero, D. Melendi, X. G. Paneda, R. Garcia, L. Pozueco, and J. L. Arciniegas, "A research on typing methods for interactive digital television applications," *IEEE Latin Amer. Trans.*, vol. 13, no. 11, pp. 3612–3620, Nov. 2015.

[3] I. S. Reljin and A. N. Sugaris, "DVB standards development," in *Proc. 9th Int. Conf. Telecommun. Modern Satell., Cable, Broadcast. Services*, Nis, Serbia, Oct. 2009, pp. 263–272.

[4] Y. Guan, Y. Dai, W. Zhang, D. Lin, and D. He, "DTMB application in Shanghai SFN transmission network," *IEEE Trans. Broadcast.*, vol. 59, no. 1, pp. 183–187, Mar. 2013.

[5] X. Zhong, L. Chen, Y. Shi, and X. Shi, "Design of multiple-polarization transmitarray antenna using rectangle ring slot elements," *IEEE Antennas Wireless Propag. Lett.*, vol. 15, pp. 1803–1806, 2016.

[6] W. Nunn and M. Figueroa, "Broad-band VSWR measurements of a Cassegrain antenna," *IEEE Trans. Antennas Propag.*, vol. AP-26, no. 6, pp. 865–867, Nov. 1978.

[7] H. Kawakami, T. Haga, S. Kon, M. Arishiro, and T. Yamashita, "Characteristics of wideband ring loop antenna for digital terrestrial broadcasting," in *Proc. IEEE Antennas Propag. Soc. Int. Symp.*, Washington, DC, USA, Jul. 2005, pp. 544–547.

[8] M. Kondo, S. Sumihiro, and G. Sato, "Two-stacked circular loop antenna for digital terrestrial TV broadcasting," in *Proc. Int. Conf. Comput. Electromagn. Appl. (ICCEA)*, Beijing, China, Nov. 1999, pp. 581–584.

[9] H. Kawakami, "A review of and new results for broadband antennas for digital terrestrial broadcasting: The modified batwing antenna," *IEEE Antennas Propag. Mag.*, vol. 52, no. 6, pp. 78–88, Dec. 2010.

[10] H. Kawakami, G. Sato, and R. Masters, "Characteristics of TV transmitting batwing antennas," *IEEE Trans. Antennas Propag.*, vol. 32, no. 12, pp. 1318–1326, Dec. 1984.

[11] H. Kawakami, T. Haga, K. Hosoi, D. Shirahama, Y. Norimatsu, Y. Ninomiya, and M. Tanioka, "Digital terrestrial broadcasting antennas - 4-Plane synthesis pattern and gain improvement-," in *Proc. IEEE Antennas Propag. Soc. Int. Symp.*, Honolulu, HI, USA, Jun. 2007, pp. 4721–4724.

[12] Y. Ojiro and H. Kawakami, "Characteristics of digital terrestrial broadcasting antennas.(2) unbalance fed modified batwing antenna," in *Proc. IEEE Antennas Propag. Soc. Int. Symp. Transmitting Waves Prog. Next Millennium, Conjunct., USNC/URSI Nat. Radio Sci. Meeting*, Salt Lake City, UT, USA, 2000, pp. 648–651.

[13] D.-J. Li, S.-J. Fang, and H.-M. Liu, "Broadband stacked antenna based on E-shaped patch for digital terrestrial TV broadcasting transmission system," in *IEEE MTT-S Int. Microw. Symp. Dig.*, Shanghai, China, Mar. 2016, pp. 1–4.

[14] Z. Lukes, K. Pitra, V. Sporik, and V. Dlouhy, "Wideband antenna for DVB-T," in *Proc. 21st Int. Conf. Radioelektronika*, Apr. 2011, pp. 1–3.

[15] K. Pitra, V. Sporik, Z. Lukes, Z. Raida, V. Dlouhy, and J. Bartyzal, "Vertically polarized antenna system for television broadcasting services," in *Proc. IEEE Int. Conf. Microw., Commun., Antennas Electron. Syst. (COMCAS)*, Tel Aviv, Israel, Nov. 2011, pp. 1–4.

[16] B. Luadang and C. Phongcharoenpanich, "Unidirectional bowtie array antenna with incision gap for digital video broadcasting-T2 base station," *IET Microw., Antennas Propag.*, vol. 9, no. 10, pp. 1087–1095, Jul. 2015.

[17] D. Casciola, G. L. Miers, and R. A. Surette, "UHF antenna choices," *IEEE Trans. Broadcast.*, vol. 45, no. 1, pp. 93–105, Mar. 1999.

[18] K. S. Vishvaksenan, K. Mithra, R. Kalaiarasan, and K. S. Raj, "Mutual coupling reduction in microstrip patch antenna arrays using parallel coupled-line resonators," *IEEE Antennas Wireless Propag. Lett.*, vol. 16, pp. 2146–2149, 2017.

[19] W. Liang, W. Zhang, D. He, Y. Guan, Y. Wang, and J. Sun, "Digital terrestrial television broadcasting in China," *IEEE Multimedia Mag.*, vol. 14, no. 3, pp. 92–97, Jul./Sep. 2007, doi: 10.1109/MMUL.2007.47.

[20] M. C. D. Maddocks, "Terrestrial TV systems and frequency planning," in *IEE Colloq. Dig.*, London, U.K., 1995, pp. 4-1–4-7.

HAIJING YU was born in Liaoning, China. She received the B.Eng. degree in information and communication engineering from Dalian Maritime University (DMU), Liaoning, China, in 2016, where she is currently pursuing the master's degree. Her current research interests include wideband antennas and passive microwave circuits.

SHAOJUN FANG (Member, IEEE) received the Ph.D. degree in communication and information systems from Dalian Maritime University (DMU), Liaoning, China, in 2001. Since 1982, he has been at DMU, where he is currently the Head Professor with the School of Information Science and Technology. He has authored or coauthored three books and over 300 journal articles and conference papers. His recent research interests include passive RF components, patch antennas, and computational electromagnetics. He was a recipient of the Best Doctor's Dissertation Award of Liaoning Province, in 2002, and the Outstanding Teacher Award of the Ministry of Transport of China.

LINGLING JIANG was born in Dalian, China. She received the B.Eng. degree in information and communication engineering from Dalian Maritime University, Liaoning, China, in 2018, where she is currently pursuing the master's degree. Her current research interests include digital television antenna and radome.

HONGMEI LIU (Member, IEEE) received the Ph.D. degree in information and communication engineering from Dalian Maritime University (DMU), Liaoning, China, in 2016. She is currently an Associate Professor with the School of Information Science and Technology, DMU. Her current research interests include CP microwave antennas, passive microwave circuits, and reconfigurable RF components. She is currently serving as a Technical Reviewer for the IEEE Transactions on Industrial Electronics, the *Electronics Letters*, and the *International Journal of RF and Microwave Computer-Aided Engineering*. She was a recipient of the Best Doctor's Dissertation Award of Liaoning Province, in 2017.